Molecular Therapy
Methods & Clinical Development
Brief Report

Mesenchymal stromal cells protect combined oncolytic and helper-dependent adenoviruses from humoral immunity

Ada Irmak Özcan,[1,6] Arianexys Aquino López,[1,2,6] Alexandra N. Wolff,[1,3] Audrey Ma,[1] Amanda Rosewell Shaw,[1,4] Masataka Suzuki,[1,5] Malcolm K. Brenner,[1,5] and Mary K. McKenna[1,5]

[1]Center for Cell Gene Therapy, Baylor College of Medicine, Texas Children's Hospital, Houston Methodist Hospital, Houston, TX 77030, USA; [2]Texas Children's Hospital, Department of Pediatrics, Houston, TX 77030, USA; [3]Harvard Medical School, Graduate School of Arts and Sciences, Boston, MA 02115, USA; [4]Benedict College, Columbia, SC 29204, USA; [5]Department of Medicine, Baylor College of Medicine, Houston, TX 77030, USA

Systemic delivery of oncolytic and immunomodulatory adenoviruses may be required for optimal effects on human malignancies. Mesenchymal stromal cells (MSCs) can serve as delivery systems for cancer therapeutics due to their ability to transport and shield these agents while homing to tumors. We now use MSCs to deliver a clinically validated binary oncolytic and helper-dependent adenovirus combination (CAdVEC) to tumor cells. We show successful oncolysis and helper-dependent virus function in tumor cells even in the presence of plasma from adenovirus-seropositive donors. In both two- and three-dimensional cultures, CAdVEC function is eliminated even at high dilutions of seropositive plasma but is well sustained when CAdVEC is delivered by MSCs. These results provide a robust *in vitro* model to measure oncolytic and helper-dependent virus spread and demonstrate a beneficial role of using MSCs for systemic delivery of CAdVEC even in the presence of a neutralizing humoral response.

INTRODUCTION

Intratumoral injection of a binary oncolytic and helper-dependent adenovirus platform (CAdVEC) has displayed clinical benefits, yielding complete responses in patients with relapsed cancer (NCT03740256).[1–3] While this study and others support the safety and utility of injecting oncolytic viruses (OVs) intratumorally, systemic administration is often preferable.[4,5] However, systemic administration is precluded by the systemic toxicity of the OV and/or by a neutralizing humoral response.[6] Using a cell carrier as a "Trojan horse" delivery system is one approach to circumvent this obstacle.[5–7]

Mesenchymal stromal cells (MSCs) offer promise as OV carrier cells due to their immune-evasive properties,[8] natural affinity to the tumor microenvironment,[9,10] and capacity to act as a site for OV replication, enabling the delivery of sufficient viral particles to the tumor site.[11–13] In addition to shielding them from neutralizing antibodies, MSCs may limit the off-target toxicity of some OVs, potentially offering safe amplification in a protective milieu.[7,13] However, whether such benefits extend to a binary system like CAdVEC remains unclear. In CAdVEC, the oncolytic component (OAd) serves a secondary purpose beyond direct tumor cell destruction by facilitating replication and amplification of a separate helper-dependent (HDAd) virus encoding immunostimulatory transgenes to boost anti-tumor immune responses.[14]

Historically, preclinical testing of OV has relied on cytotoxic activity in conventional two-dimensional (2D) cell culture and subsequently in animal studies. Here, we adopted a modified liquid overlay technique in an ultralow attachment plate to generate 3D cultures that produce consistent tumor spheroids. These spheroids are amenable to CAdVEC infection, enabling us to replicate both solid tumor dimensionality and pre-existing immunity *in vitro*.[15,16] Using this model, we demonstrate that CAdVEC-infected MSCs infiltrate solid tumors to disseminate both oncolytic and immunostimulatory components, and that infectious particles resisted neutralization by plasma from AdV-seropositive donors.

RESULTS

NSCLC cell lines and MSCs are infected with CAdVEC

To trace infection and expression of both components of CAdVEC in our *in vitro* systems, we used an OAd expressing red fluorescent protein (RFP) and HDAd expressing green fluorescent protein (GFP).[2] Previous studies showed optimal transgene expression in both tumor and MSCs with a combination of OAd serotype 5 and an HDAd with 5/3 chimeric fiber/knob.[17] Thus, we infected MSCs with 100 vp/cell OAd.5-RFP and 1,000 vp/cell HDAd.5/3-GFP and imaged them 24 h post infection (Figure 1A). We confirmed that MSCs produced functional marker transgenes by adding MSC supernatant to a

Received 26 February 2024; accepted 4 June 2024;
https://doi.org/10.1016/j.omtm.2024.101279.

[6]These authors contributed equally

Correspondence: Mary K. McKenna, Center for Cell Gene Therapy, Baylor College of Medicine, Texas Children's Hospital, Houston Methodist Hospital, Houston, TX 77030, USA.
E-mail: mary.mckenna@bcm.edu

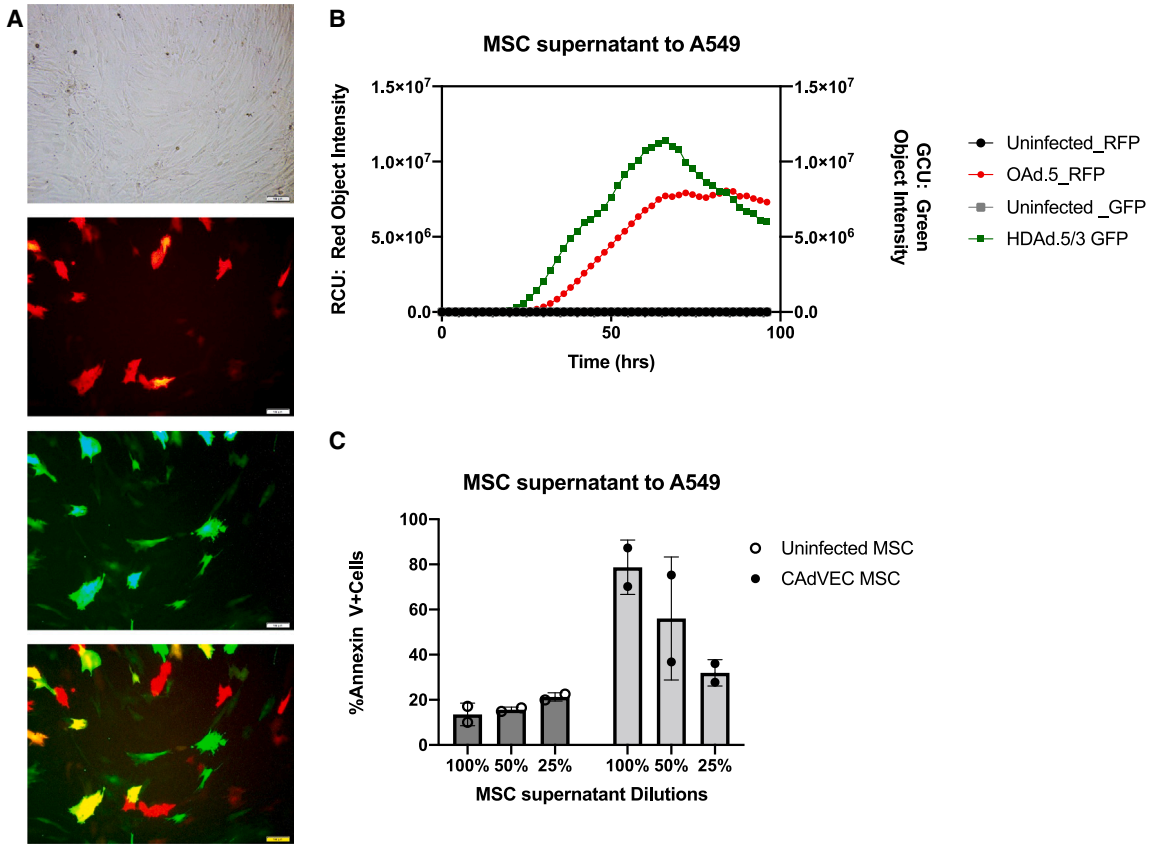

Figure 1. Bone-marrow-derived MSCs are susceptible to CAdVEC infection

(A) Bright-field and fluorescent microscopy images of MSCs infected with 100 vp/cell OAd.5 and 1,000 vp/cell HDAd.5/3 expressing RFP and GFP respectively 48 h post infection. (B) RFP expression (left axis) and GFP expression (right axis) of A549 cells incubated with 96 h CAdVEC MSC supernatant. Red object intensity (RCU) and green object intensity (GCU) measured by IncuCyte Live image analysis over time. (C) Supernatant was collected from CAdVEC MSCs 96 h post infection and added to A549 cells. Cell death measured by annexin V staining via flow cytometry of A549 tumor cells treated with dilutions of CAdVEC MSC supernatant (technical replicates) 96 h later to confirm OAd-mediated oncolysis. Error bars represent standard deviation.

monolayer of the non-small cell lung cancer (NSCLC) cell line A549 (Figure 1B) that resulted in oncolysis of target cells (Figure 1C).

Neutralizing plasma proteins block direct CAdVEC infection

To test how pre-existing humoral immunity influences the ability of CAdVEC to infect tumor cells and mimic systemic delivery of the virus, we measured the expression of CAdVEC in the NSCLC lines A549 and H1650 in conventional 2D cultures containing plasma collected from AdV-seropositive donors. Since plasma may contain elements that either enhance or diminish AdV infection,[18,19] we tested the overall effects of donor plasma rather than inhibition by gamma globulin fraction alone.

We incubated 100 vp/cell of OAd.5-RFP and 1,000 vp/cell of HDAd.5/3-GFP in pure PBS or the indicated plasma dilutions for 1 h and then added them to A549 and H1650 cells. PBS controls produced the greatest signal of both RFP (OAd.5) and GFP (HDAd.5/3) in both cell lines, followed by a dose-dependent reduction of transgene expression with the diluted plasma (Figure 2A). When lower doses of CAdVEC were used to infect the tumor cells at the same OAd:HDAd ratio (10 vp/cell OAd.5-RFP and 100 vp/cell HDAd.5/3-GFP) 1:10 plasma dilution was sufficient to eliminate both OAd and HDAd transgene expression, and even a 1:100 plasma dilution significantly reduced production of both transgenes (Figures 2B and 2C and Video S1).

We repeated this study in 3D tumor spheroids and obtained similar results. We observed strong expression of both RFP and GFP in the PBS control, indicating that both CAdVEC components infect tumor spheroids. At 100 vp/cell OAd.5-RFP and 1,000 vp/cell HDAd.5/3-GFP, we saw strong neutralization with the 1:10 and 1:100 dilutions of plasma, similar to our 2D models. These results confirm that pre-existing immunity blunts even infection with high viral loads (Figure 2D). Similarly, with lower doses of virus, all three dilutions of plasma reduced transgene expression in tumor spheroids (Figures 2E and 2F and Video S2). These results show that plasma proteins neutralize naked CAdVEC virus in both conventional 2D culture and 3D tumor spheroids.

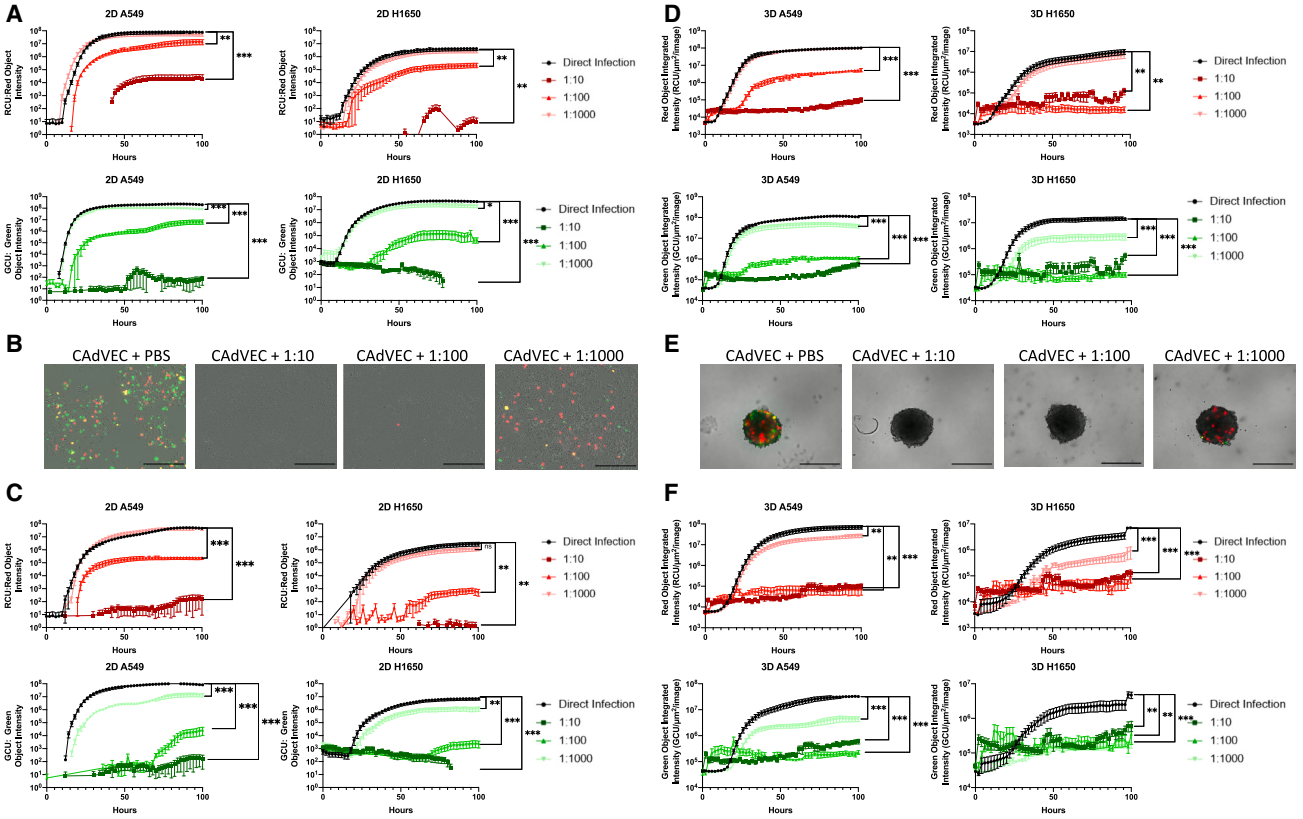

Figure 2. Direct CAdVEC infection is neutralized by plasma proteins of healthy donors

CAdVEC only or direct infection conditions are incubated with PBS as a control. (A) 2D A549 and H1650 tumor cells were infected with a high dose of 100 vp/cell OAd.5 and 1,000 vp/cell HDAd.5/3 expressing RFP (top) and GFP (bottom) measured by IncuCyte Live imaging over time. (B) IncuCyte images of A549 cells infected with a low-dose 10 vp/cell OAd.5 and 100 vp/cell HDAd.5/3 at 96 h with or without dilutions of plasma. (C) RFP (top) and GFP (bottom) expression in 2D A549 and H1650 tumor cells with low-dose infection over time. (D) High-dose CAdVEC infection in 3D tumor spheroids. RFP and GFP expressions were measured by IncuCyte Live imaging over time in both A549 and H1650 tumor spheroids with different dilutions of plasma. (E) IncuCyte images of 3D A549 tumor spheroids post infection of low-dose 10 vp/cell OAd.5 and 100 vp/cell HDAd.5/3 expressing RFP and GFP respectively at 96 h with different dilutions of plasma. (F) RFP and GFP expression in 3D A549 and H1650 tumor spheroids infected with low-dose CAdVEC. Scale bar represents 400 μM. p values are signified by asterisks: $^{*}p < 0.05$, $^{**}p < 0.01$, ** $^{*}p < 0.001$ determined by unpaired Student's t test at 100 h; n = 9–12 replicates. Data are presented as means +/− SEM.

MSCs shield CAdVEC from neutralization in both 2D and 3D cultures

Next, we assessed the ability of MSCs to shield AdV from neutralization in the presence of seropositive donor plasma. 24 h after infection, CAdVEC MSCs were incubated for 1 h with either PBS or plasma (at the indicated dilutions) before being added to monolayer cultures of NSCLC cells (Figure 3). In the absence of plasma, MSCs delivered CAdVEC to tumor cells, with increased RFP and GFP signal intensity over time. In the presence of seropositive plasma, however, the signals remained primarily within the MSCs with minimal spread to tumor cells (Figures 3A and 3B and Video S3).

However, we observed a different pattern in 3D tumor spheroid cultures. CAdVEC MSCs incubated with PBS alone showed the expected increase in OAd- and HDAd-derived transgenes (Figures 3C and 3D and Video S4). Addition of seropositive plasma, however, increased both RFP and GFP expression in tumor spheroids compared to PBS control, and this increase was greater at the 1:10 dilution of plasma. These results indicate that plasma can enhance the expression of viral transgenes when the viruses are delivered by MSCs (Figure S1). Thus, while seropositive plasma inhibited direct CAdVEC infection in spheroids, it significantly improved infection by CAdVEC in MSCs (Figure 3E).

Next, we tested how increasing the concentration of plasma affected the increased transgene expression by CAdVEC MSCs. Whether we used 10% or 90% plasma dilutions, results in our 3D model were similar (Figure S2). Overall, these findings indicate that MSC delivery of CAdVEC may not only shield virus from neutralization by seropositive plasma, but it also may augment CAdVEC delivery due to interaction with the co-factors in plasma known to assist AdV survival and infectivity.[18]

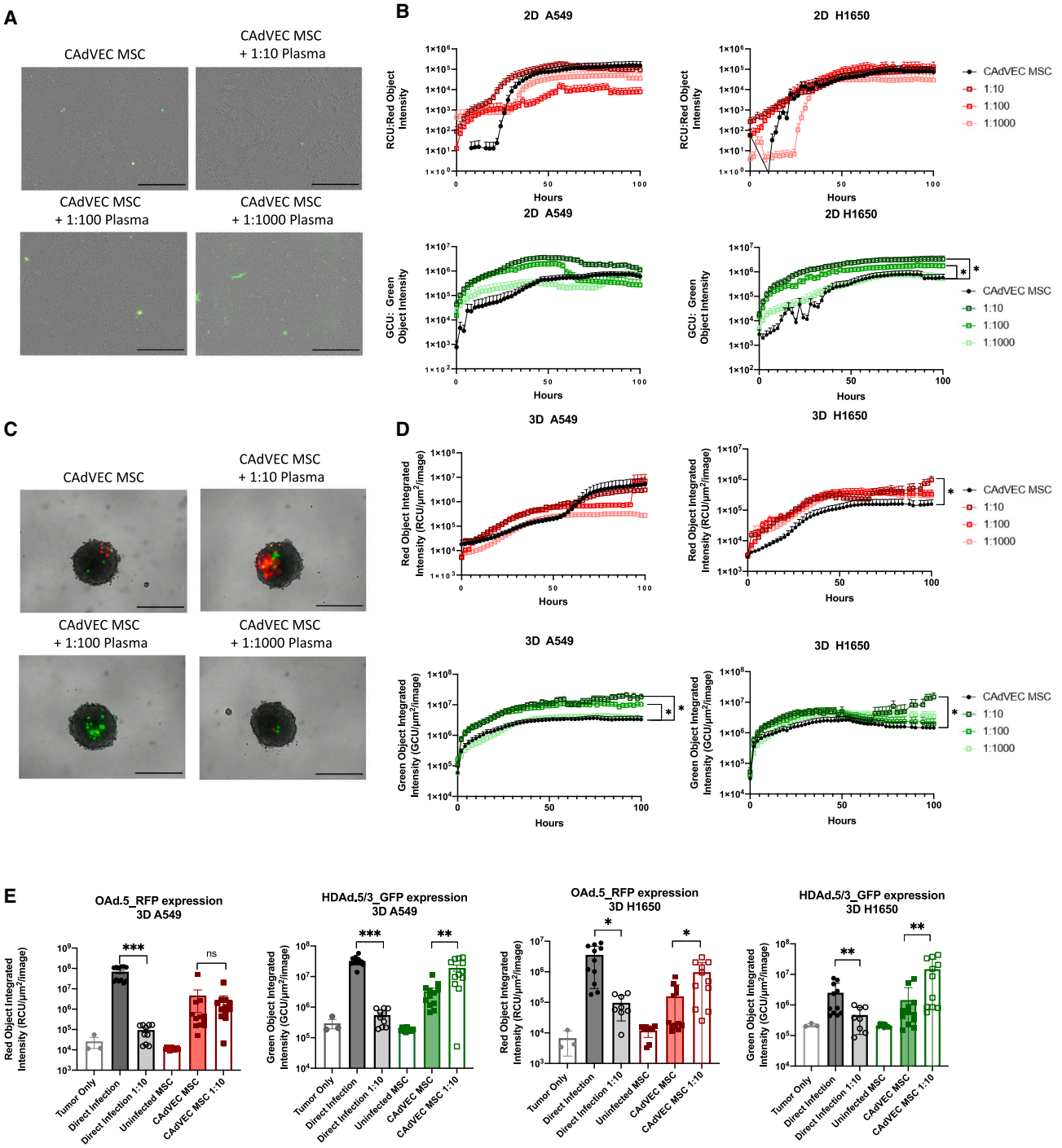

Figure 3. CAdVEC MSCs shield virus from neutralization in both 2D and 3D culture settings

MSCs were infected with 100 vp/cell OAd.5_RFP and 1,000 vp/cell HDAd.5/3_GFP. 24 h later, CAdVEC MSCs were incubated in either PBS or diluted plasma for 1 h and then delivered to a tumor cultured in 2D and 3D settings. (A) Representative IncuCyte images of 2D culture of A549 cells at 96 h post addition. (B) Quantification of OAd.5_RFP (top) and HDAd.5/3_GFP (bottom) in 2D culture over time. Fluorescence was measured by object intensity within the IncuCyte software. (C) Images of A549 tumor spheroids 96 h after CAdVEC MSC delivery with different dilutions of neutralizing plasma. (D) Quantification of OAd.5_RFP (top) and HDAd.5/3_GFP (bottom) in 3D culture over time.

(legend continued on next page)

DISCUSSION

Here, we demonstrate that MSCs infected with CAdVEC provide protection against neutralization by pre-existing plasma proteins in 3D tumor spheroid models. We evaluated virus spread via marker transgenes and found that MSCs can deliver both CAdVEC components. Further, seropositive plasma enhanced viral-mediated transduction in our 3D spheroids, a phenomenon not observed in 2D cultures. Thus, MSCs shield low doses of CAdVEC to maintain efficacy while remaining well within levels shown to be safe for each component of the combination therapy in preclinical and clinical studies.[1,17,20]

CAdVEC, designed to compensate for the limited cargo capacity of oncolytic AdV, utilizes HDAds, allowing for incorporation of multiple transgenes. Co-infection of malignant cells by CAdVEC components initiates HDAd replication, amplifying HDAd-encoded transgenes. Understanding the vulnerability of each CAdVEC component to neutralization by pre-existing immunity is crucial, as antibodies and other immune responses are a primary defense.[6,21] This model highlights how humoral immunity interacts with MSC-mediated CAdVEC delivery, though it was not designed to evaluate adaptive cellular immunity. In the future, more comprehensive *in vitro* models, such as incorporating virus-specific T cells in 3D spheroids to assess their impact on CAdVEC spread, coupled with studies in vaccine-immunized humanized mice, will be needed to validate these results.

Overall, these findings demonstrate that MSCs can shield OVs from immune evasion mechanisms. In 3D tumor cultures, seropositive plasma paradoxically enhances CAdVEC transduction when delivered by MSCs, likely due to plasma components, like factor X, that promote transduction while interfering with neutralization.[22,23] This suggests a benefit from plasma proteins in AdV-seropositive individuals to improve CAdVEC infection.[19,21] Thus, our data support the feasibility of using MSCs to shield CAdVEC from humoral immune responses, enabling its safe systemic delivery to tumor sites. Compared to 2D cultures, 3D cultures provide valuable insights into MSC and CAdVEC function in the presence of AdV seropositivity, facilitating preclinical optimization of the approach.

MATERIALS AND METHODS

CAdVEC infection of cell lines and MSCs

A549 and H1650 cell lines were previously obtained from ATCC. MSCs were isolated from healthy donors as previously described.[24] Both OAd.5 and HDAd.5/3 expressing RFP and GFP were produced as we previously described.[2] MSCs were infected as previously described.[17]

3D tumor spheroid generation

We seeded 2×10^3 tumor cells on 1% agarose coated plates as previously described[25,26] and confirmed spontaneous spheroid formation by microscope visualization at 48 h. MSCs were added at a 1:200 MSC-to-tumor cell ratio. IncuCyte imaging with "Brand" default 96-well plate setting was used. Uncalibrated images were exported and uploaded to NIH ImageJ software for image processing and visualization.

Neutralization assay

We collected blood from healthy donors through an institutional review board (IRB)-approved protocol using heparin-coated vacutainers, centrifuged it at $500 \times g$ for 15 min, and heat-inactivated the plasma at 56°C for 30 min and then stored it at −20°C. Plasma was diluted in sterile PBS. Seropositivity for OAd.5 and HDAd.5/3 was confirmed in three donors (Figure S3). For infection controls, we calculated and prepared the necessary viral particles, diluting them in PBS or plasma, and incubated them at 37°C for 1 h. For neutralization studies with CAdVEC MSC, we collected and counted MSCs 24 h post infection, resuspending them in PBS or diluted plasma.

IncuCyte image analysis

Green object intensity (GCU) and red object intensity (RCU) parameters were used for analysis for 2D culture. For 3D culture, multispheroid protocol was used for image acquisition and quantified by using total red object integrated intensity and total green object integrated intensity parameters. Non-transduced tumor cells were used as control wells for background fluorescent masking, and 8% red signal was subtracted from green signal for spectral unmixing.

Statistics

Statistical analyses were performed using GraphPad Prism, with data normality assessed by the Anderson-Darling test. Significance was set at $p < 0.05$, with asterisks indicating levels of significance ($^*p < 0.05$, $^{**}p < 0.01$, $^{***}p < 0.001$) and "ns" denoting no significant difference.

DATA AND CODE AVAILABILITY

The data that supports these findings are available from the corresponding author (M.K.M.) upon request.

SUPPLEMENTAL INFORMATION

Supplemental information can be found online at https://doi.org/10.1016/j.omtm.2024.101279.

ACKNOWLEDGMENTS

Special thanks to Dr. Tao Wang with the Dan L Duncan Comprehensive Cancer Center for her support and expertise in statistical analyses. We'd also like to thank the BCM Integrated Microscopy Core and CPRIT-funded GCC Center for Advanced Microscopy and Image Informatics (RP170719).

Fluorescence measured by object integrated intensity within the IncuCyte software ($n = 4$ wells/condition). p value calculated at the 100-h time point. (E) Quantification of 96-h time point in 3D culture of A549 (left) and H1650 (right) comparing direct infection with CAdVEC MSC delivery ($n = 3$ MSC donors in quadruplicate) in the presence of 1:10 plasma dilution, indicated by "1:10." Scale bar represents 400 μM. p values are signified by asterisks: $^*p < 0.05$, $^{**}p < 0.01$, $^{***}p < 0.001$ determined by unpaired Student's t test. Data are presented as means +/− SEM.

This project was supported by the National Heart, Lung, and Blood Institute of the National Institutes of Health under award number 5T32HL092332-17 (PI: Dr. Helen Heslop) and the National Cancer Institute under the award 5PO1CA094237-15.

AUTHOR CONTRIBUTIONS

Conceptualization, M.K.M. and M.K.B.; investigation, M.K.M., A.I.O., A.A.L., A.W., A.M., and A.R.S.; formal analysis, M.K.M., A.I.O., A.A.L., A.W., and A.M.; writing – original draft, M.K.M.; writing – review and editing, M.K.M., A.R.S., and M.K.B.; supervision, A.R.S., M.S., and M.K.B.; funding acquisition, M.K.B.

DECLARATION OF INTERESTS

M.K.B. serves on advisory boards for Marker Therapeutics, Allogene, Walking Fish, Abintus, Athenex-Kuur, Onk Therapeutics, Coya Therapeutics, Triumvira, Adaptimmune, Vor Therapeutics, and Tscan. M.K.B has equity in Allovir, Tessa Therapeutic Ltd, and Marker Therapeutics. M.K.B. has royalties from Takeda and Bellicum. M.S. received research funding from Tessa Therapeutic Ltd. and AstraZeneca. M.S. was a scientific consultant for Tessa Therapeutic Ltd.

REFERENCES

1. Wang, D., Porter, C.E., Lim, B., Rosewell Shaw, A., Robertson, C.S., Woods, M.L., Xu, Y., Biegert, G.G.W., Morita, D., Wang, T., et al. (2023). Ultralow-dose binary oncolytic/helper-dependent adenovirus promotes antitumor activity in preclinical and clinical studies. Sci. Adv. *9*, eade6790. https://doi.org/10.1126/sciadv.ade6790.
2. Farzad, L., Cerullo, V., Yagyu, S., Bertin, T., Hemminki, A., Rooney, C., Lee, B., and Suzuki, M. (2014). Combinatorial treatment with oncolytic adenovirus and helper-dependent adenovirus augments adenoviral cancer gene therapy. Mol. Ther. Oncolytics *1*, 14008. https://doi.org/10.1038/mto.2014.8.
3. Rosewell Shaw, A., Porter, C.E., Watanabe, N., Tanoue, K., Sikora, A., Gottschalk, S., Brenner, M.K., and Suzuki, M. (2017). Adenovirotherapy Delivering Cytokine and Checkpoint Inhibitor Augments CAR T Cells against Metastatic Head and Neck Cancer. Mol. Ther. *25*, 2440–2451. https://doi.org/10.1016/j.ymthe.2017.09.010.
4. Havunen, R., Santos, J.M., Sorsa, S., Rantapero, T., Lumen, D., Siurala, M., Airaksinen, A.J., Cervera-Carrascon, V., Tähtinen, S., Kanerva, A., and Hemminki, A. (2018). Abscopal Effect in Non-injected Tumors Achieved with Cytokine-Armed Oncolytic Adenovirus. Mol. Ther. Oncolytics *11*, 109–121. https://doi.org/10.1016/j.omto.2018.10.005.
5. Ferguson, M.S., Lemoine, N.R., and Wang, Y. (2012). Systemic delivery of oncolytic viruses: hopes and hurdles. Adv. Virol. *2012*, 805629. https://doi.org/10.1155/2012/805629.
6. Groeneveldt, C., van den Ende, J., and van Montfoort, N. (2023). Preexisting immunity: Barrier or bridge to effective oncolytic virus therapy? Cytokine Growth Factor Rev. *70*, 1–12. https://doi.org/10.1016/j.cytogfr.2023.01.002.
7. Wang, X., Zhao, X., and He, Z. (2021). Mesenchymal stem cell carriers enhance antitumor efficacy of oncolytic virotherapy. Oncol. Lett. *21*, 238. https://doi.org/10.3892/ol.2021.12499.
8. Ankrum, J.A., Ong, J.F., and Karp, J.M. (2014). Mesenchymal stem cells: immune evasive, not immune privileged. Nat. Biotechnol. *32*, 252–260. https://doi.org/10.1038/nbt.2816.
9. Nwabo Kamdje, A.H., Kamga, P.T., Tagne Simo, R., Vecchio, L., Seke Etet, P.F., Muller, J.M., Bassi, G., Lukong, E., Goel, R.K., Amvene, J.M., and Krampera, M. (2017). Mesenchymal stromal cells' role in tumor microenvironment: involvement of signaling pathways. Cancer Biol. Med. *14*, 129–141. https://doi.org/10.20892/j.issn.2095-3941.2016.0033.
10. Almeida-Porada, G., Atala, A.J., and Porada, C.D. (2020). Therapeutic Mesenchymal Stromal Cells for Immunotherapy and for Gene and Drug Delivery. Mol. Ther. Methods Clin. Dev. *16*, 204–224. https://doi.org/10.1016/j.omtm.2020.01.005.
11. Ghaleh, H.E.G., Vakilzadeh, G., Zahiri, A., and Farzanehpour, M. (2023). Investigating the potential of oncolytic viruses for cancer treatment via MSC delivery. Cell Commun. Signal. *21*, 228. https://doi.org/10.1186/s12964-023-01232-y.
12. Moreno, R. (2021). Mesenchymal stem cells and oncolytic viruses: joining forces against cancer. J. Immunother. Cancer *9*, e001684. https://doi.org/10.1136/jitc-2020-001684.
13. Ghasemi Darestani, N., Gilmanova, A.I., Al-Gazally, M.E., Zekiy, A.O., Ansari, M.J., Zabibah, R.S., Jawad, M.A., Al-Shalah, S.A.J., Rizaev, J.A., Alnassar, Y.S., et al. (2023). Mesenchymal stem cell-released oncolytic virus: an innovative strategy for cancer treatment. Cell Commun. Signal. *21*, 43. https://doi.org/10.1186/s12964-022-01012-0.
14. Biegert, G.W.G., Rosewell Shaw, A., and Suzuki, M. (2021). Current development in adenoviral vectors for cancer immunotherapy. Mol. Ther. Oncolytics *23*, 571–581. https://doi.org/10.1016/j.omto.2021.11.014.
15. Fitzgerald, A.A., Li, E., and Weiner, L.M. (2020). 3D Culture Systems for Exploring Cancer Immunology. Cancers *13*, 56. https://doi.org/10.3390/cancers13010056.
16. Han, S.J., Kwon, S., and Kim, K.S. (2021). Challenges of applying multicellular tumor spheroids in preclinical phase. Cancer Cell Int. *21*, 152. https://doi.org/10.1186/s12935-021-01853-8.
17. McKenna, M.K., Englisch, A., Brenner, B., Smith, T., Hoyos, V., Suzuki, M., and Brenner, M.K. (2021). Mesenchymal stromal cell delivery of oncolytic immunotherapy improves CAR-T cell antitumor activity. Mol. Ther. *29*, 1808–1820. https://doi.org/10.1016/j.ymthe.2021.02.004.
18. Allen, R.J., and Byrnes, A.P. (2019). Interaction of adenovirus with antibodies, complement, and coagulation factors. FEBS Lett. *593*, 3449–3460. https://doi.org/10.1002/1873-3468.13649.
19. Cheneau, C., and Kremer, E.J. (2020). Adenovirus-Extracellular Protein Interactions and Their Impact on Innate Immune Responses by Human Mononuclear Phagocytes. Viruses *12*, 1351. https://doi.org/10.3390/v12121351.
20. Ruano, D., López-Martín, J.A., Moreno, L., Lassaletta, Á., Bautista, F., Andión, M., Hernández, C., González-Murillo, Á., Melen, G., Alemany, R., et al. (2020). First-in-Human, First-in-Child Trial of Autologous MSCs Carrying the Oncolytic Virus Icovir-5 in Patients with Advanced Tumors. Mol. Ther. *28*, 1033–1042. https://doi.org/10.1016/j.ymthe.2020.01.019.
21. Jayawardena, N., Poirier, J.T., Burga, L.N., and Bostina, M. (2020). Virus-Receptor Interactions and Virus Neutralization: Insights for Oncolytic Virus Development. Oncolytic Virotherapy *9*, 1–15. https://doi.org/10.2147/OV.S186337.
22. Xu, Z., Qiu, Q., Tian, J., Smith, J.S., Conenello, G.M., Morita, T., and Byrnes, A.P. (2013). Coagulation factor X shields adenovirus type 5 from attack by natural antibodies and complement. Nat. Med. *19*, 452–457. https://doi.org/10.1038/nm.3107.
23. Findlay, J.S., Cook, G.P., and Blair, G.E. (2018). Blood Coagulation Factor X Exerts Differential Effects on Adenovirus Entry into Human Lymphocytes. Viruses *10*, 20. https://doi.org/10.3390/v10010020.
24. Hoyos, V., Del Bufalo, F., Yagyu, S., Ando, M., Dotti, G., Suzuki, M., Bouchier-Hayes, L., Alemany, R., and Brenner, M.K. (2015). Mesenchymal Stromal Cells for Linked Delivery of Oncolytic and Apoptotic Adenoviruses to Non-small-cell Lung Cancers. Mol. Ther. *23*, 1497–1506. https://doi.org/10.1038/mt.2015.110.
25. Lv, D., Hu, Z., Lu, L., Lu, H., and Xu, X. (2017). Three-dimensional cell culture: A powerful tool in tumor research and drug discovery. Oncol. Lett. *14*, 6999–7010. https://doi.org/10.3892/ol.2017.7134.
26. Thomsen, A.R., Aldrian, C., Bronsert, P., Thomann, Y., Nanko, N., Melin, N., Rücker, G., Follo, M., Grosu, A.L., Niedermann, G., et al. (2017). A deep conical agarose microwell array for adhesion independent three-dimensional cell culture and dynamic volume measurement. Lab Chip *18*, 179–189. https://doi.org/10.1039/c7lc00832e.